

Synchrony affects Taylor's law in theory and data

Daniel C. Reuman^{a,b,c,1}, Lei Zhao^{a,b}, Lawrence W. Sheppard^{a,b}, Philip C. Reid^{d,e,f}, and Joel E. Cohen^{c,g,h,i,1}

^aDepartment of Ecology and Evolutionary Biology, University of Kansas, Lawrence, KS 66045; ^bKansas Biological Survey, University of Kansas, Lawrence, KS 66047; ^cLaboratory of Populations, Rockefeller University, New York, NY 10065; ^dThe Laboratory, Sir Alister Hardy Foundation for Ocean Science, Plymouth PL1 2PB, United Kingdom; ^eMarine Institute, Plymouth University, Plymouth PL4 8AA, United Kingdom; ^fThe Laboratory, Marine Biological Association of the United Kingdom, Plymouth PL1 2PB, United Kingdom; ⁹The Earth Institute, Columbia University, New York, NY 10027; ^hDepartment of Statistics, Columbia University, New York, NY 10027; and Department of Statistics, University of Chicago, Chicago, IL 60637

Contributed by Joel E. Cohen, May 4, 2017 (sent for review March 6, 2017; reviewed by Michael J. Plank and Xiao Xiao)

Taylor's law (TL) is a widely observed empirical pattern that relates the variances to the means of groups of nonnegative measurements via an approximate power law: variance $a \approx a \times \text{mean}_a^b$, where g indexes the group of measurements. When each group of measurements is distributed in space, the exponent b of this power law is conjectured to reflect aggregation in the spatial distribution. TL has had practical application in many areas since its initial demonstrations for the population density of spatially distributed species in population ecology. Another widely observed aspect of populations is spatial synchrony, which is the tendency for time series of population densities measured in different locations to be correlated through time. Recent studies showed that patterns of population synchrony are changing, possibly as a consequence of climate change. We use mathematical, numerical, and empirical approaches to show that synchrony affects the validity and parameters of TL. Greater synchrony typically decreases the exponent b of TL. Synchrony influenced TL in essentially all of our analytic, numerical, randomization-based, and empirical examples. Given the near ubiquity of synchrony in nature, it seems likely that synchrony influences the exponent of TL widely in ecologically and economically important systems.

fluctuation scaling | mean variance scaling | Moran effect | correlation | aphid

aylor's law (TL) is a widely observed empirical pattern that relates the variances to the means of groups of measurements of population densities or other nonnegative quantities via a power law: variance_g $\approx a \times \text{mean}_g^b$, where g indexes the groups of measurements, a > 0, b is usually positive, and a and b are both independent of g. Equivalently, $\log(\text{variance}_g) \approx b \times \log(\text{mean}_g) +$ log(a). The parameter b has the same numerical value regardless of whether it appears as the exponent of the power law or the slope of the linear relation between log(variance,) and $log(mean_g)$. Thus, b may be referred to as the exponent or the slope of TL.

TL has been verified in data on the population sizes and population densities of hundreds of taxa, including aphids (1), crops (2), fish (3, 4), birds (5), and humans (6). TL has also been discovered in many other nonnegative measurements (7), including recently, tornados per outbreak (8) and stocks (9). In physics, TL is sometimes called "fluctuation scaling." TL has been generalized (10) and applied or proposed for application to fisheries management (3, 4), estimation of species persistence times (11), and agriculture (2, 12, 13). Potential mechanisms of TL have been explored extensively (9, 14, 15). Because of its ubiquity, it has been suggested that TL could be another "universal law," like the central limit theorem (16).

There are multiple versions of TL, "Temporal TL" and "spatial TL," on which we focus, use time series, $Y_i(t)$, of population densities measured in locations i = 1, ..., n at times t = 1, ..., nT. For temporal TL, the groups, g, consist of all measurements made in a location, i (means and variances are computed over time). For spatial TL, groups are measurements at a single time, t (means and variances are over space).

Synchrony (metapopulation synchrony, spatial synchrony) is another ubiquitous and fundamental ecological phenomenon. It is the tendency for time series of population densities of the

same species measured in geographically separated locations to be correlated through time. It has been observed in organisms as diverse as protists (17), insects (18), mammals (19, 20), and birds (21; ref. 22 has many other examples). It relates to large-scale pest or disease outbreaks and shortages of resources (23, 24) and has implications for conservation because populations are at greater risk of simultaneous extinction if they are simultaneously rare (24).

Although some empirical and theoretical connections have been made between synchrony and TL (7, 14, 20, 25), the connections are far from completely understood and do not encompass all versions of TL. Synchrony, like TL, may reflect aggregation, because the spatial extent of correlations among population time series indicates the geographic size of outbreaks (26). Engen, et al. (25) connected TL with synchrony theoretically but did not use spatial or temporal TL. Temporal TL has been related to a kind of synchrony that occurs on spatial scales smaller than that of sampling (7, 14).

The "Moran effect" refers to synchrony caused by synchronous environmental drivers. Changes in Moran effects as a consequence of climate change may alter synchrony. Long-term increases in the synchrony of caribou populations in Greenland were associated with increases in the synchrony of environmental drivers in the area, apparently through modified Moran effects (19). The latter were, in turn, linked to global warming. Similar associations held for North American bird species (21). Large-scale climatic changes in the North Atlantic Oscillation caused changes in winter temperature synchrony, which in turn caused changes in the synchrony of pest aphid species in the United Kingdom (27). Changes in the synchrony of plankton (26) and tree rings (28) have been associated with climate change. If synchrony influences TL,

Significance

Two widely confirmed patterns in ecology are Taylor's law (TL), which states that the variance of population density is approximately a power of mean population density, and population synchrony, the tendency of species' population sizes in different areas to be correlated through time. TL has been applied in many areas, including fisheries management, conservation, agriculture, finance, physics, and meteorology. Synchrony of populations increases the likelihood of large-scale pest or disease outbreaks and shortages of resources. We show that changed synchrony modifies and can invalidate TL. Widespread recent changes in synchrony, possibly resulting from climate change, may broadly affect TL and its applications.

Author contributions: D.C.R. and J.E.C. designed research; D.C.R., L.Z., L.W.S., and J.E.C. performed research; D.C.R., L.Z., L.W.S., P.C.R., and J.E.C. contributed new reagents/ analytic tools; D.C.R., L.Z., and L.W.S. analyzed data; and D.C.R., L.Z., and J.E.C. wrote

Reviewers: M.J.P., University of Canterbury; and X.X., University of Maine.

The authors declare no conflict of interest.

¹To whom correspondence may be addressed. Email: reuman@ku.edu or cohen@ rockefeller.edu.

This article contains supporting information online at www.pnas.org/lookup/suppl/doi:10. 1073/p nas. 1703593114/-/DCS up ple me ntal

then changes in synchrony may change TL in ecologically and economically important systems.

We analyze connections between synchrony and spatial TL to answer the following questions. Do the presence and strength of synchrony in population time series influence whether TL holds and if so, how? Do the presence and strength of synchrony influence the slope b of TL and if so, how? Because of the fundamental importance of both TL and synchrony to population ecology, illuminating connections between these phenomena is of intrinsic interest, but we are also motivated by the applied importance of TL and concern that climate change may modify synchrony.

Results

Analytic Results. Suppose the population size or density in location i at time t is modeled by the nonnegative random variable $Y_i(t)$ for i = 1, ..., n. Assume that the multivariate stochastic process $Y(t) = (Y_1(t), ..., Y_n(t))$ is stationary and ergodic (29); these assumptions are standard (SI Appendix, S1). We use the standard spatial sample mean and sample variance: $m(t) = (1/n)\sum_{i=1}^{n} Y_i(t)$ and $v(t) = \sum_{i=1}^{n} Y_i(t)^2/(n-1) - nm(t)^2/(n-1)$. The traditional plot to test spatial TL is the $\log(v(t))$ vs. $\log(m(t))$ scatterplot for a finite realization of these processes. TL hypothesizes that this plot will be approximately linear. The linear regression slope is $b_t = cov_t(\ln(m(t)), \ln(v(t)))/var_t(\ln(m(t)))$ (30). The subscripts t indicate that the variance var_t and the covariance cov_t are computed across time for the finite realization, whereas each value of m(t) and v(t) is computed across space at time t. A standard (22) measure of average synchrony, $\Omega_t = (1/n^2) \sum_{i,j=1}^n cor_t(Y_i(t), Y_j(t))$, averages the temporal correlations of the standard of the tions of every pair of population dynamic time series. This summation includes the terms with i = j, which equal 1, and hence Ω_t is 1/n when the correlations with $i \neq j$ are 0; Ω_t is zero when the spatial average time series is constant, and Ω_t cannot be negative (SI Appendix, S1). We are interested in how Ω_t may affect whether the relationship between the log mean and the log variance is linear and the value of the slope b_t when linearity holds. For long time series, it suffices (SI Appendix, S1) to consider the population quantities $b = cov(\ln(m), \ln(v))/var(\ln(m))$ and $\Omega = (1/n^2) \sum_{i,j=1}^{n} cor(Y_i, Y_j)$, assuming that all of the expectations, variances, and covariances in these expressions and others exist (details are in *SI Appendix*). Thus, we work with the time-independent distribution $Y = (Y_1, ..., Y_n)$. Autocorrelation in time series will not influence the relationships that we study if time series are long enough for empirical and true marginal distributions to be similar (SI Appendix, S1).

Applying the delta method (31), $\ln(m) \approx \ln(E(m)) + (m - E(m))/E(m)$, $\ln(v) \approx \ln(E(v)) + (v - E(v))/E(v)$, and $var(\ln(m)) \approx var(m)/E(m)^2$; therefore (SI Appendix, SI)

$$b \approx \frac{(n-1)E(m)}{n} \frac{cov(m,v)}{(A-var(m))var(m)},$$
 [1]

where the first factor in this expression and the quantity $A = (1/n)\sum_{i=1}^n \mathrm{E}(Y_i^2) - \mathrm{E}(m)^2$ depend solely on the marginal distributions, Y_i , and do not depend on the correlations, $cor(Y_i, Y_j)$. However, var(m) equals $(1/n^2)\sum_{i,j=1}^n cov(Y_i, Y_j)$, which relates to synchrony, Ω , and is similar in form. Eq. 1, therefore, provides the intuition behind our subsequent analyses: if synchrony $[\Omega]$ or var(m) changes and the marginals, Y_i , remain fixed, then one expects the slope b to change. The following theorem supports this intuition.

Theorem. Suppose Y_i are identically distributed (but not necessarily independent) with $E(Y_i) = M > 0$ and finite $var(Y_i) = V > 0$. Assume that $\mu_{ij} = E((Y_i - M)(Y_j - M))$, $\mu_{ijk} = E((Y_i - M)(Y_j - M)(Y_k - M))$, and $\mu_{ijkl} = E((Y_i - M)(Y_j - M)(Y_k - M)(Y_l - M))$ are finite for all i, j, k, and k, and define $\rho_{ij} = cor(Y_i, Y_j) = \mu_{ij}/V$ and $\rho_{ijk} = \mu_{ijk}/\mu_{iii}$. Then

$$b \approx \left(\frac{M\mu_{iii}}{V^2}\right) \left(\frac{\sum_{i,j=1}^n \rho_{ijj} - \frac{1}{n} \sum_{i,j,k=1}^n \rho_{ijk}}{n^2 (1 - \Omega)\Omega}\right).$$
[2]

The approximation is better whenever the coefficients of variation of the sample mean $\sqrt{var(m)}/E(m) = \sqrt{V\Omega}/M$ and sample variance $\sqrt{var(v)}/E(v)$ are smaller, and is asymptotically perfect as these quantities approach zero.

Additional details, alternative mathematically equivalent expressions for b, and a proof of the theorem are in SI Appendix, S2.

This theorem extends a theorem by Cohen and Xu (15), which assumes that the Y_i are independent and identically distributed (iid). In that case, the second factor on the right of Eq. 2 is 1, and $b \approx (M\mu_{iii}/V^2)$, which equals the skewness $\mu_{iii}/V^3/^2$ of Y_i divided by its coefficient of variation $V^{1/2}/M$. Independence of the Y_i is not necessary here: the same formula holds if $\rho_{ij} = 0$ for $i \neq j$ and $\rho_{ijk} = 0$ whenever i, j, and k are not all equal. Cohen and Xu (15) concluded that, in the iid case, skewness of Y_i is necessary and sufficient for TL to have slope $b \neq 0$. Our theorem extends this result to the case of identically distributed Y_i that may be nonindependent.

The denominator $n^2(1-\Omega)\Omega$ in Eq. 2 is a \cap -shaped function of Ω (i.e., it increases, has a maximum, and then decreases again as Ω increases). Therefore, Eq. 2 may seem to suggest that b is a U-shaped function of synchrony (it decreases, has a minimum, and then increases again). However, the numerator of the second factor of Eq. 2 may, a priori, also be a \cap -shaped function of synchrony; therefore, a \cup -shaped dependence of b on synchrony is not mathematically certain, and neither are any of the components of such a dependence (the initial decrease, the internal minimum, and the subsequent increase of b as Ω increases). Dependence of the numerator of Eq. 2 on Ω also means that $\lim_{\Omega \to 0} b$ and $\lim_{\Omega \to 1} b$ can be finite, although $\lim_{\Omega \to 0} (1-\Omega)\Omega$ and $\lim_{\Omega \to 1} (1-\Omega)\Omega$ are 0.

Numerical Results. To illustrate the identically distributed case, we performed numerical simulations based on multivariate normal random variables $X=(X_1,\ldots,X_n)$ with mean $(0,\ldots,0)$ and covariance matrix with diagonal entries 1 and off-diagonal entries equal to a parameter, $\rho \geq 0$. We let $Y_i = \varphi(X_i)$, where the transformations $\varphi(.)$ were chosen, in different simulations, to make the Y_i a variety of Poisson, negative binomial, gamma, exponential, χ^2 , normal, and log-normal distributions. Increases in ρ produced increases in Ω . Exponential and χ^2 distributions are special cases of gamma distributions. We produced separate results for these distributions because they are widely used. Results are in SI Appendix, S3; Fig. 1 shows typical results for Poisson and gamma examples.

Results generally agreed with the above intuitions and analyses. The linearity hypothesis of TL was usually, but not always, an adequate approximation in that linearity and homoscedasticity could not be rejected statistically (SI Appendix, S6 has details on how this was tested). In agreement with our theorem and Cohen and Xu (15), when a shifted normal distribution (which has skewness 0) was used for Y_i , $b \approx 0$ for all values of Ω . For skewed distributions, the slope b was generally smaller for larger values of Ω , confirming the prediction that b depends on synchrony. Although b decreased steeply as Ω increased from zero for all skewed distributions, b most commonly continued to decrease monotonically as Ω increased further, even for large values of Ω , except for a few cases using gamma distributions, for which modest increases were observed (SI Appendix, Figs. S14-S20): the b vs. synchrony relationship was only occasionally \cup -shaped, and then only mildly so. The right side of Eq. 2 was computed analytically (i.e., with formulas) for gamma, exponential, χ^2 , normal, and log-normal examples, and the formulas were compared with numerical results. For some distributions and parameters, the approximation was very accurate, and it was always at least qualitatively accurate (in the sense that it showed similar

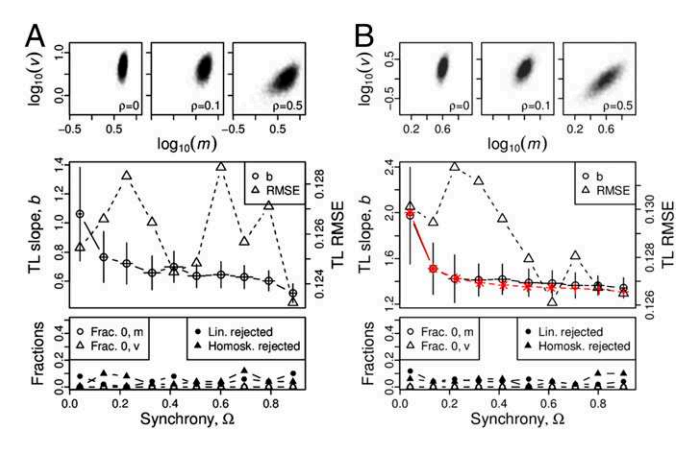


Fig. 1. Effects of spatial synchrony on spatial TL for a model with populations identically distributed in different sampling locations and iid through time at each location. Examples use (A) Poisson ($\lambda = 5$) and (B) gamma (shape $\alpha = 8$, rate $\beta = 2$) distributions (SI Appendix, S3 shows the parameterization of the gamma distribution). (Top) m is spatial sample mean and v is spatial sample variance. Confirming TL visually, approximately linear $log_{10}(v)$ vs. $log_{10}(m)$ relationships held with selected values of ρ . Slopes were shallower for greater synchrony. (Middle) TL had a shallower slope for greater synchrony. Black lines show the average (across 50 simulations) TL slope plotted against average synchrony (error bars are standard deviations) and average (over 50 simulations) of the root mean squared errors (RSME) of $log_{10}(v)$ values from $log_{10}(v)$ vs. $log_{10}(m)$ linear regressions (labeled TL RMSE in the axis label). (B) Red lines are analytic approximations (Eq. 2 and Theorem 5 in SI Appendix, S2.3), computable with readily available software for continuous distributions (SI Appendix, S3), with + and \times symbols indicating points for which approximations were deemed adequate via two different methods, respectively; both symbols are plotted when both methods indicate an adequate approximation. Each simulation consisted of 25 populations sampled 100 times each. (Bottom) Fractions of m and v values, which were 0 and therefore ignored, and fractions of 50 simulations, for which statistical tests rejected linearity or homoskedasticity of the $\log_{10}(v)$ vs. $\log_{10}(m)$ relationship with 95% confidence. Frac, fraction; Homosk, homoskedasticity; Lin, linearity. SI Appendix, Figs. S1-S32 show other parameters and distributions, which often showed similar patterns. Additional details are in SI Appendix, S3 and S6.

declines of b with increasing synchrony), except for the lognormal distribution, for which it was very inaccurate for some parameters because of insufficient sampling as previously observed (15). As expected from the theorem, Eq. 2 was a better approximation for smaller Ω .

We also constructed nonidentically distributed examples by applying transformations to multivariate normal random variables. Our theorem, which assumed identically distributed Y_i , did not apply here. The random variable X was the same as above, and $Y_i = \varphi_i(X_i)$, where the $\varphi_i(.)$ differed for different i. The $\varphi_i(.)$ values were chosen so that all of the Y_i were from the same family (Poisson, negative binomial, gamma, exponential, χ^2 , normal, or log normal), although with different parameters. For gamma, normal, exponential, and log-normal examples, the $\varphi_i(.)$ were chosen so that Y_i was distributed in the same way as (but was not equal to) f_iY_1 , where $0 < f_1 < \ldots < f_n$. This procedure was not possible for negative binomial, Poisson, or χ^2 distributions because these families are not closed under multiplication by positive real numbers. Distributions used for these families and the results are described in SI Appendix, S4.

Results reinforced most of the generalities that emerged from the above analytical results and simulations, although a \cup -shaped dependence of b on Ω was more common and stronger in these examples (SI Appendix, S4). Exceptions to general tendencies did occur. For gamma, exponential, normal, and log-normal examples, TL was usually a good approximation. Although linearity was often statistically rejected, departures from linearity were modest: $\log(\nu)$ vs. $\log(m)$ plots stayed very close to the regression line. The slope b always showed an initial steep decrease as Ω increased

from zero for all gamma, exponential, normal, and log-normal examples. As $\Omega \rightarrow 1$, these examples approached the case for which Y_i equals f_iY_1 almost surely in addition to having the same distribution as f_iY_1 . In that limit, $m = \text{mean}_i(Y_i) = \text{mean}_i(f_iY_1) =$ Y_1 mean_i (f_i) , whereas $v = var_i(Y_i) = var_i(f_iY_1) = Y_1^2 var_i(f_i)$. Therefore, TL should hold exactly with slope two. This argument holds even for symmetric distributions like the normal. Our numerical simulations confirmed that, as Ω increased toward one, root mean squared errors from $\log(v)$ vs. $\log(m)$ regressions went to zero, and b went to two, sometimes from above and sometimes from below. An approach from below was paired with U-shaped dependence of b on Ω , which was common and often pronounced in these examples. The earlier result (15) that skewness is required for TL to have slope $b \neq 0$ if Y_i are identically distributed does not hold when Y_i are not identically distributed: simulations with Y_i normally distributed had $b \neq 0$ (SI Appendix, Figs. S45–S50). For Poisson and χ^2 examples, TL was usually a reasonable approximation, and b declined steeply as Ω increased from zero and continued to decrease for larger Ω . Negative binomial examples often strongly violated TL, especially for large values of Ω (e.g., SI Appendix, Figs. S63 and S64). Nonetheless, the slope b tended to decrease with increasing Ω whenever linearity held approximately.

Another way to create families of random variables Y with fixed marginal distributions but varying synchrony is based on sums of independent random variables representing local and regional influences on populations (32). It is well-known that, for independent Poisson random variables X and X_i , the sum $X + X_i$ is Poisson distributed. Similar facts are also true for the negative binomial, gamma, and normal families. Therefore, Y was generated by setting $Y_i = X + X_i$ for independent X and X_i for i = 1, ..., n. The variable X can be interpreted as the influence of a large-spatial-scale environmental or other factor that affects all populations; the X_i are local effects. Different relative variances of X and the X_i led to different amounts of correlation (synchrony) among the Y_i . By this approach, we constructed Y, such that the Y_i were identically distributed according to a desired Poisson, negative binomial, gamma, exponential, χ^2 , or normal distribution, with a desired level of synchrony among the Y_i . Details of this construction and the results are in SI Appendix, S5.

Results were the same in some respects as the results above and differed in others. Larger values of synchrony always decreased the slope b (except for normal Y_i , for which b was always zero as expected from the theorem because Y_i are again identically distributed). The slope b went to zero as Ω approached one. The approximation Eq. 2 applied reasonably accurately. In all cases, the right side of Eq. 2 reduced to simple, monotonically decreasing functions of Ω . However, contrary to prior simulations, log(v) vs. log(m) plots often strongly violated the linear hypothesis of TL. Values of synchrony Ω larger than zero smeared points rightward in log(v) vs. log(m) space, destroying the linear relation expected from TL. This smearing decreased b but also changed its meaning from representing the slope of a linear pattern to representing the slope of a linear approximation to a nonlinear pattern. The decrease in b did not reflect maintenance of a linear pattern with a changed slope as in prior examples (Fig. 1 and SI Appendix, S3 and S4). SI Appendix,

Empirical Results. We examined the influence of synchrony on empirical data using 82 spatiotemporal population datasets. The datasets included annual time series of population density for 20 species of aphid sampled for 35 y in 11 locations across the United Kingdom, annual density time series for 22 plankton groups sampled in 26 regions in the seas around the United Kingdom for 56 y, and chlorophyll-a density time series measured at several locations at each of 10 depths in four distance categories from the coast of southern California over 28 y. We henceforth refer to distance categories from shore in the chlorophyll-a data as groups 1–4, where group 1 refers to the closest

S5 gives an explanation for this effect.

Reuman et al. PNAS Early Edition | 3 of 6

category to shore and larger group numbers correspond to farther categories from shore. *Methods* has additional descriptions

of the data and their processing.

The spatial TL was reasonably well-supported by all 82 datasets. SI Appendix, Figs. S91–S96 plots $\log(v)$ vs. $\log(m)$ and gives statistical tests of TL. Conformity to TL was not perfect, but quite good overall, except for the chlorophyll-a data in group 3 (SI Appendix, Fig. S95). Linearity or homoskedasticity of the $\log(v)$ vs. $\log(m)$ relationship was rejected at the 1% level for 7 of 82 datasets (1 aphid species, 1 depth from group 1, and 5 depths from group 3).

We examined correlations across species, taxonomic groups, or depths (for the aphid, plankton, and chlorophyll-a datasets, respectively) between measurements of b and Ω . Factors other than synchrony may have influenced these results and are accounted for below after examining the raw correlations here. Fig. 2A, D, G, J, M, and P shows that b and Ω were significantly negatively correlated across aphid species and across depths in the chlorophyll-a data, groups 1 and 2, and nonsignificantly negatively correlated across plankton groups in the plankton data. Higher synchrony Ω was associated with lower slope b in these data, despite possible confounding influences.

However, significant positive correlations occurred in the chlorophyll-a data, groups 3 and 4 (Fig. 2 M and P). These positive associations seem to conflict with simulation results, which generally support a negative association between b and Ω , unless confounding factors overwhelmed a negative influence of synchrony on b in these data. For instance, changes across depths in b may be influenced for the chlorophyll-a data, groups 3 and 4, by changes across depths in Ω and possible changes in time series marginal distributions. Simulations carried out above held time series marginal distributions constant when synchrony was varied.

To control for changes in time series marginal distributions that may have occurred in concert with changes in synchrony, we decomposed slopes $b = b_{\text{marg}} + b_{\text{sync}}$ into contributions due to synchrony, b_{sync} , and due to time series marginals, b_{marg} . We computed the marginal contribution, b_{marg} , by independently randomizing time series and then recomputing the log(v) vs. log(m)slope (Methods) to eliminate synchrony and ensure that it cannot contribute to b_{marg} . Then, we defined b_{sync} as $b - b_{\text{marg}}$. Fig. 2 C, F, I, L, O, and R shows that b_{sync} was negatively associated with Ω in all cases (albeit not always significantly), even for chlorophyll-a data, groups 3 and 4 (Fig. 2 O and R). For these groups, b_{marg} was strongly positively associated with Ω (Fig. 2 N and Q). This positive association overwhelmed the negative association of b_{sync} with Ω to produce the overall positive association of b with Ω observed in Fig. 2 M and P. Thus, groups 3 and 4 results did not conflict with simulation results, but rather showed that other factors dominated. The change in time series marginal distributions for the chlorophyll-a data was not surprising, because these data were gathered across different depths, and chlorophyll-a density varies with depth in the ocean. SI Appendix, Fig. S99 is like Fig. 2 but identifies the species/groups/depths of plotted points; panels for the chlorophyll-a data show that depth probably played a role. Differing thermocline depths across groups 1-4 (SI Appendix, Fig. S101) may also have been important.

To examine in more detail the influence of synchrony on spatial TL in empirical data, we performed additional randomizations (*Methods*). Randomizations reduced or increased the synchrony in each of our 82 spatiotemporal population datasets while not modifying the marginal distributions in each sampling location. In virtually every case, increasing synchrony decreased b, whereas decreasing synchrony increased b (Fig. 3). The strength of the effect varied across datasets and was typically steeper for smaller values of synchrony. Values of b_{marg} correspond to the y-axis intercepts of the curves in Fig. 3. In a few cases, b appeared to depend in a \cup -shaped way on synchrony, as in some simulations, but the \cup shape was modest when it occurred, also in agreement with simulations (i.e., only modest

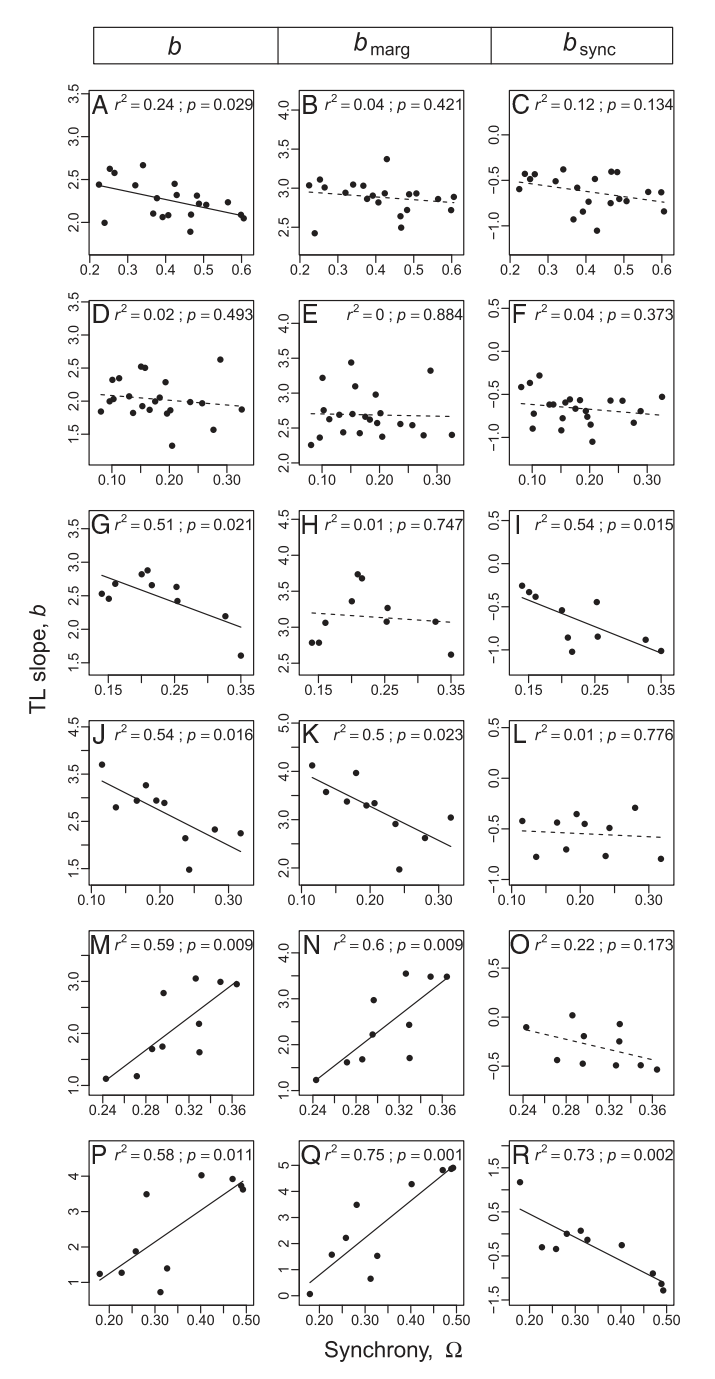


Fig. 2. Plots of TL slope b against synchrony Ω for (A) 20 species of a phid in the United Kingdom, (D) 22 plankton groups in the seas around the United Kingdom, and (G, J, M, and P) chlorophyll-a density time series measured at 10 depths in groups 1–4 (Methods), which are distance categories from shore. A, D, G, J, M, and P are paired with contributions to the slope, b, of <math>(B, E, H, K, N, and Q) marginal distribution structure (b_{marg}) and (C, F, I, L, O, and R) synchrony (b_{sync}) , respectively (Methods). Associations between synchrony and TL slope b can be due to associations between synchrony and b_{marg} , associations between synchrony and b_{sync} , or both, because $b = b_{\text{marg}} + b_{\text{sync}}$. SI Appendix, Fig. S99 shows another version of the figure that labels individual species/groups/depths.

increases in b with increasing Ω were observed in Fig. 3 B, D, and F). The linearity of TL was approximately supported across the range of synchrony values, except possibly for the highest synchrony values and the chlorophyll-a data in group 3 (SI Appendix, Figs. S97 and S98).

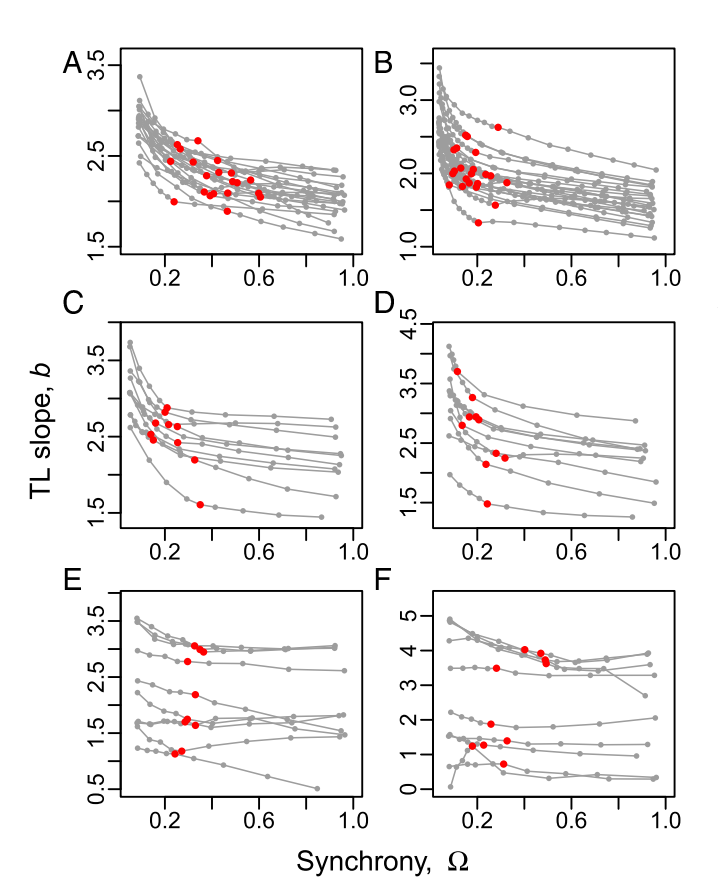


Fig. 3. The dependence of the spatial TL slope b on synchrony Ω , where synchrony was manipulated through randomizations or sorting of time series (Methods) for (A) aphid species, (B) plankton groups, and (C-F) a chlorophylla density index measured at 10 depths. C is for 19 group-1 locations, F is for 12 group-4 locations, and D and E are for 12 locations in each of two intermediate distance categories (groups 2 and 3) (Methods). Red points on plotted lines correspond to individual unrandomized (A) aphid species, (B) plankton groups, and (C-F) sampling depths detailed in SI Appendix, Table 51. Gray points are averages over randomizations or sortings (Methods). Values for individual randomizations are shown in SI Appendix, Fig. 5100.

All results are summarized, with hyperlinks to supporting figures and derivations, in SI Appendix, Tables S3 and \$4.

Discussion

Understanding the relationship of synchrony with TL is important, because both patterns are widespread in population ecology, and because TL and recent observed climate changeinduced modifications in synchrony have applied importance

We showed that the strength of synchrony substantially influences the log(variance) vs. log(mean) scatterplot, of which TL is one special form. It can destroy linearity of TL, but more commonly, it preserves linearity and changes the slope b of the plot. Synchrony influenced the slope of TL in essentially all of our analytic, numerical, empirical, and randomization-based examples. The one systematic exception occurred when the marginal distributions of time series in different locations were normally and identically distributed, so that a nonzero slope of TL was not expected with or without synchrony (15). As synchrony increased from zero, slope b almost always decreased quite sharply. For some theoretical and randomization examples, increasing synchrony starting from higher levels of synchrony increased the slope b modestly, but analogous increases were not seen in empirical examples when confounding changes in time series marginal distributions were controlled. Our analytic results generalize a theorem of Cohen and Xu (15). We provided a simple method

of decomposing b into its contributions due to synchrony, b_{sync} ,

and due to time series marginal distributions, b_{marg} .

Ballantyne and Kerkhoff (14) and Eisler, et al. (section 3 in ref. 7) described interesting links between small-spatial-scale synchrony and temporal TL. To explain the basic idea, we construct an idealized example using aphids monitored by suction traps. Suppose trap i for i = 1, ..., n has A_i agricultural fields that can produce aphids within its sampling range. Suppose traps are placed so that no fields contribute to more than one trap. Suppose field ij $(i = 1, ..., n; j = 1, ..., A_i)$ contributes a random variable $V_{ij}(t)$ to trap i in year t, and suppose all of the $V_{ij}(t)$ are identically distributed with mean μ and variance σ^2 . Then, if, for fixed i, $V_{ij}(t)$ are perfectly correlated so that all fields near i produce the same number of sampled aphids per year (this assumption constitutes very strong small-spatial-scale synchrony, the spatial scale being smaller than the spatial resolution of sampling), the mean of the number of aphids $\sum_{i} V_{ij}(t)$ sampled by trap i in year t is $\mu_i = A_i \times \mu$, and the variance is $\sigma_i^2 = A_i^2 \times \mu$ σ^2 . Assuming that random variables for different times t are independent, the mean and variance across time of numbers of aphids sampled by trap i will converge almost surely, in the limit of long time series, to these same values (strong law of large numbers). Log transforming and doing basic algebra give $\ln(\sigma_i^2) = 2 \times$ $ln(\mu_i) + C_1$ for a constant C_1 ; this equation demonstrates a temporal TL with slope two. If, for fixed i, $V_{ij}(t)$ are independent, then the mean of $\sum_{j} V_{ij}(t)$ is again $\mu_i = A_i \times \mu$, but the variance is now $\sigma_i^2 = A_i \times \sigma^2$. Log transforming and doing basic algebra give temporal TL with slope one. (This example shows, incidentally, that observing TL with slope one need not be evidence that the aphids or other organisms are Poisson distributed, although Poisson-distributed aphids or other organisms lead to TL with

The above example differs in at least two important ways from our results. First, it concerns temporal TL, whereas we studied spatial TL. Second, the above example concerns synchrony at a different spatial scale from our study. Although dependence between numbers of aphids sampled at different traps seems likely to imply dependence between numbers contributed by fields within the range of individual traps, the reverse need not

It seems worthwhile, in future research, to examine the possibly complex relationships between the above example (7, 14) and our study. Although Eisler, et al. (7) focus on temporal TL, they state without proof or details that many of their results also apply to TL more generally. Relationships between spatial and temporal TL have recently been examined (20) and may help connect the TL in the above example to the spatial TL of our study. Perhaps all of these versions of TL could be formally related to each other and synchrony.

Engen, et al. (25) produced a general model for analyzing a version of TL, in which each group of measurements of population density comes from plots of the same size, but different groups use different plot sizes (distinct from spatial and temporal TL). On p. 2,620 in ref. 25, they remind the reader that increasing population migration leads to increasing synchrony, which causes "the slope [of this version of TL] ... to increase from 1 to 2 ... as the migration increases." Engen, et al. (25) seem to indicate in the final sentences of their paper that their model could be extended to address spatial TL, possibly helping to illuminate connections among spatial, temporal, and their versions of TL and synchrony.

Cohen and Saitoh (20) examined relationships among synchrony and spatial and temporal TL in voles. Their example is consistent with our work and illustrates the value of our general results for understanding TL in specific systems. Using 31 y of population density data for the gray-sided vole, Myodes rufocanus, at 85 locations in Hokkaido, Japan, Cohen and Saitoh (20) verified that spatial and temporal TL held for the data as well as simulations of a previously validated Gompertz model of the dynamics of these populations. However, simulated time series had spatial and temporal TL slopes substantially steeper than

Reuman et al. PNAS Early Edition | 5 of 6 those from data. Cohen and Saitoh (20) observed that most pairs of vole populations were significantly temporally correlated and modified the Gompertz model accordingly. When densityindependent perturbations in model dynamics were synchronized, inducing synchrony in simulated population time series, and when simulated populations with higher mean density had a reduced variance of density-independent perturbations, the modeled slopes of spatial and temporal TL were reduced to values similar to those of the data. Our results here account qualitatively for the effect on TL slopes of the first of these two modifications of the Gompertz model (i.e., the introduction of synchrony).

Our theoretical models and our randomizations kept the marginal distributions of time series fixed as synchrony changed to exclude confounding factors. In our empirical analyses, we identified the contribution of synchrony, b_{sync} , to the empirical TL slope b. In reality, synchrony may change jointly with marginal distributions across species, or depths, or some other axis of variation, as in some of our empirical data (Fig. 2). Covariation between changes in b_{sync} and b_{marg} should be context-dependent, may be biologically revealing, and is worth examining when multiple values of b are computed.

Increasing evidence shows that changing Moran effects, possibly due to climate change, modify synchrony (19, 21, 26–28). This work indicates that changed synchrony will modify the slope and possibly the validity of TL, with ramifications for applications of TL in many areas, including resource management (3), conservation (11), human demography (6), tornado outbreaks (8), and agriculture (2, 12, 13). Given the ubiquity of synchrony in nature (22), it seems highly likely that synchrony often affects values of TL slopes in real populations, as Hokkaido voles showed. It is important to understand better how TL is affected by synchrony and other factors.

Methods

Analytic and Numerical Methods. Full details of analytic results are in 5/ Appendix, S1 and S2, and full details of numerical simulations are in SI Appendix, S3-S6.

Data. The Rothamsted Insect Survey runs a network of suction traps that sample flying aphids. Daily aphid counts are collected throughout the flight season for many species at multiple locations. Data were processed to produce annual total counts for 20 species (SI Appendix, Table S1) at 11 locations (SI Appendix, Table S2) for the years 1976–2010, forming 20 spatiotemporal population datasets.

- 1. Taylor LR (1961) Aggregation, variance and the mean. Nature 189:732-735.
- 2. Döring TF, Knapp S, Cohen JE (2015) Taylor's power law and the stability of crop yields. Field Crops Res 183:294-302.
- 3. Kuo TC, Mandal S, Yamauchi A, Hsieh CH (2016) Life history traits and exploitation affect the spatial mean-variance relationship in fish abundance. Ecology 97:
- 4. Xu M, Kolding J, Cohen JE (2017) Taylor's power law and fixed precision sampling: Application to abundance of fish sampled by gillnets in an African lake. Can J Fish Aquat Sci 74:87-100.
- 5. Taylor LR, Perry JN, Woiwod IP, Taylor RAJ (1988) Specificity of the spatial power-law exponent in ecology and agriculture. Nature 332:721–722.
- Cohen JE, Xu M, Brunborg H (2013) Taylor's law applies to spatial variation in a human population. Genus 69:25-60.
- 7. Eisler Z, Bartos I, Kertész J (2008) Fluctuation scaling in complex systems: Taylor's law and beyond. Adv Phys 57:89-142.
- 8. Tippett MK, Cohen JE (2016) Tornado outbreak variability follows Taylor's power law of fluctuation scaling and increases dramatically with severity. Nat Commun 7:10668.
- 9. Fronczak A, Fronczak P (2010) Origins of Taylor's power law for fluctuation scaling in complex systems. Phys Rev E Stat Nonlin Soft Matter Phys 81:066112.
- 10. Giometto A, Formentin M, Rinaldo A, Cohen JE, Maritan A (2015) Sample and population exponents of generalized Taylor's law. Proc Natl Acad Sci USA 112:7755-7760.
- Kalyuzhny M, et al. (2014) Temporal fluctuation scaling in populations and communities. Ecology 95:1701–1709.
- 12. Bechinski EJ. Pedigo LP (1981) Population dispersion and development of sampling plans for Orius insidiosus and Nabis spp. in soybeans. Environ Entomol 10:956-959.
- Kogan M, Ruesink WG, McDowell K (1974) Spatial and temporal distribution patterns of the bean leaf beetle, $\it Cerotoma\ trifur\ Cata$ (Forester), on soybeans in Illinois. $\it Environ$ Entomol 3:607-617.
- 14. Ballantyne F, 4th, Kerkhoff AJ (2005) Reproductive correlation and mean-variance scaling of reproductive output for a forest model. J Theor Biol 235:373-380.
- 15. Cohen JE, Xu M (2015) Random sampling of skewed distributions implies Taylor's power law of fluctuation scaling. Proc Natl Acad Sci USA 112:7749-7754.

The Continuous Plankton Recorder survey, now operated by the Sir Alister Hardy Foundation for Ocean Science, has sampled the seas around the United Kingdom for plankton abundances since before World War II using a sampling device towed behind commercial ships. Data were processed to produce annual abundance time series for 22 phytoplankton and zooplankton taxa (SI Appendix, Table S1) for 26 $2^{\circ} \times 2^{\circ}$ areas around the United Kingdom for the years 1958-2013, forming 22 spatiotemporal population datasets.

The California Cooperative Oceanic Fisheries Investigations have surveyed the California Current System since 1949, measuring chlorophyll-a regularly since 1984. Time series of spring chlorophyll-a were based on measurements at 55 sites, which were divided into four groups based on distance from shore, with group 1 near to shore (average 87.7 km) and group 4 far from shore (average 539.3 km). For each site and sampling occasion, annual chlorophyll abundances were calculated for 0-, 10-, 20-, 30-, 50-, 75-, 100-, 125-, 150-, and 200-m depths, forming 10 spatiotemporal datasets for each group.

Additional data details are in SI Appendix, S7.

Randomizations and the Decomposition of b. Given a $T \times n$ matrix, with each column containing a time series of population size or density from one location (therefore, T is the length of the time series and n is the number of sampling locations), synchrony was reduced without affecting time series marginal distributions for the sampling locations by selecting k rows randomly and then randomly replacing the entries in those rows with randomly chosen (with replacement) values from the same column; this replacement was done independently within each column. Larger values of k destroy a larger fraction of any synchrony that was originally present in the time series. Setting k = T completely eliminates synchrony by randomizing each complete time series independently. To increase the synchrony, starting from the original time series, k rows were again selected randomly. Within each column of this $k \times n$ submatrix separately, entries were sorted into increasing order. For each value of k, k rows were selected randomly in 100 ways, with values of b and Ω averaged for Fig. 3. The value b_{marg} was computed by randomizing time series with k = T as described above to destroy synchrony and then computing $b = b_{\text{marg}}$ for the randomized dataset.

ACKNOWLEDGMENTS. We thank contributors to the Continuous Plankton Recorder and the California Cooperative Oceanic Fisheries Investigations datasets; D. Stevens and P. Verrier for data extraction; J. Walter and T. Anderson for helpful suggestions; and Priscilla K. Rogerson for assistance. We also thank the staff of the Rothamsted Insect Survey (RIS), particularly James Bell. The RIS is a National Capability funded by Biotechnology and Biological Sciences Research Council. D.C.R., L.Z., and L.W.S. were partially supported by the University of Kansas, including Tier II and General Research Fund grants, as well as the James S. McDonnell Foundation. D.C.R. was partially supported by US National Science Foundation (NSF) Grant 1442595. J.E.C. was partially supported by NSF Grant DMS-1225529.

- 16. Jørgensen B (1997) The Theory of Dispersion Models (Chapman & Hall, London).
- 17. Holyoak M, Lawler SP (1996) Persistence of an extinction-prone predator-prey interaction through metapopulation dynamics. Ecology 77:1867-1879.
- 18. Hanski I, Woiwod IP (1993) Spatial synchrony in the dynamics of moth and aphid populations. J Anim Ecol 62:656-668.
- 19. Post E, Forchhammer MC (2004) Spatial synchrony of local populations has increased in association with the recent Northern Hemisphere climate trend. Proc Natl Acad Sci USA 101:9286-9290
- $20. \ \ Cohen\, JE, Saito\, h\, T\, (2016)\, Population\, dynamics, synchrony,\, and\, environmental\, quality$ of Hokkaido voles lead to temporal and spatial Taylor's laws. Ecology 97:3402-3413.
- 21. Koenig WD, Liebhold AM (2016) Temporally increasing spatial synchrony of North American temperature and bird populations. Nat Clim Chang 6:614-617
- 22. Liebhold A, Koenig WD, Bjørnstad ON (2004) Spatial synchrony in population dynamics. Annu Rev Ecol Evol Syst 35:467-490.
- 23. Micheli F, et al. (1999) The dual nature of community variability. Oikos 85:161–169.
- 24. Earn DJD, Levin SA, Rohani P (2000) Coherence and conservation. Science 290:
- 25. Engen S, Lande R, Sæther BE (2008) A general model for analyzing Taylor's spatial scaling laws. Ecology 89:2612-2622.
- 26. Defriez EJ, Sheppard LW, Reid PC, Reuman DC (2016) Climate change-related regime shifts have altered spatial synchrony of plankton dynamics in the North Sea, Glob Change Biol 22:2069-2080
- 27. Sheppard LW, Bell JR, Harrington R, Reuman DC (2016) Changes in large-scale climate alter synchrony of aphid pests. Nat Clim Chang 6:610-613.
- Shestakova TA, et al. (2016) Forests synchronize their growth in contrasting Eurasian regions in response to climate warming. Proc Natl Acad Sci USA 113:662-667.
- 29. Brillinger DR (2001) Time Series: Data Analysis and Theory (SIAM, Philadelphia)
- 30. Snedecor G, Cochran W (1980) Statistical Methods (Iowa State Univ Press, Ames, IA), 7th Ed
- 31. Oehlert GW (1992) A note on the delta method. Am Stat 46:27-29
- 32. Fischer CH (1933) On correlation surfaces of sums with a certain number of random elements in common. Ann Math Stat 4:103–126.